Published in "Dalton Transactions 45(4): 1504–1513, 2016"
which should be cited to refer to this work.

N-Nitrosamine-{*cis*-Re[CO]$_2$}$^{2+}$ cobalamin conjugates as mixed CO/NO-releasing molecules†

Giuseppe Santoro,[a] Ruben Beltrami,[b] Emmanuel Kottelat,[b] Olivier Blacque,[a] Anna Yu. Bogdanova[c] and Fabio Zobi*[b]

Mixed CO/NO-releasing molecules were prepared by conjugation of the 17-electron rhenium dicarbonyl *cis*-[Re(CO)$_2$Br$_4$]$^{2-}$ complex to *N*-nitrosamine modified cyanocobalamin (B12) bio-vectors. The species were fully characterized by standard analytical techniques, including X-ray crystallography for cyanocobalamin-5′-*O*-pyrazine and (**1**) and its *N*-pyrazine nitrosylated derivative (**1a**). The *N*-nitrosamine B12 derivatives are able to liberate low NO doses in buffer solutions and appear to be "activated" towards NO release if in contact with cultured cells. Coordination of the *cis*-[Re(CO)$_2$Br$_4$]$^{2-}$ complex on the axial cyanide of B12 allows for the combined loss of CO and NO from the conjugates. The mixed CO/NO-releasing molecules show cytoprotection in an ischemia–reperfusion model but no significant enhanced synergistic effects over the relative NORMs and CORMs building constituents.

Introduction

Nitric oxide (NO) and carbon monoxide (CO) are established gasotransmitters involved in multiple signalling pathways in cells and tissues. NO is formed enzymatically as a product of L-arginine cleavage by NO synthases (NOS) and upon non-enzymatic reduction of NO_2^- by deoxygenated haemoglobin and myoglobin. CO is produced during the degradation of heme by heme oxygenases (HOs). Crucial importance of NO and CO for living organisms was confirmed by the studies of HOs and NOS in knockout mice. Biochemical parallels between the two gases are particularly striking in the circulation and nervous system where both NO and CO may function as co-transmitters in the same neurons.[1,2] Strong evidence supports the notion that interactions of CO and NO may influence the physiological responses to each of these gases at the enzyme biosynthetic level *via* a positive feedback loop mechanism whereby NO elevates the levels of heme oxygenase-1 mRNA and protein,[3–5] and CO increases the steady state level of NO.[6] Uncoupling or dysregulation of NO and CO production results in severe pathologies such as oncotransformation, hypertension, chemoreception, cardiovascular diseases *etc.*[7–9]

Restoration of NO/CO bioavailability upon exhaustion of their pools in diseased tissues may be achieved by administration of NO and CO releasing molecules.[10,11] Nitric oxide releasing molecules (NORMs) have been used for more than 100 years for therapeutic use.[12–14] More recently, CORMs (CO releasing molecules) have been the subject of intense scrutiny.[15–20] Like their nitric oxide-releasing counterparts, CORMs are pro-drugs that upon activation release therapeutic doses of carbon monoxide and display beneficial effects in *e.g.* atherosclerosis, vascular constriction, inflammation, cellular protection, hyperoxia-induced injury, and other physiological situations.[21] In light of the akin biological roles of NO and CO, synergistic cytoprotective effects of two gases might be expected. Indeed these were demonstrated in an acute hepatic and vascular injury model.[22,23] Intrigued by these reports, we hypothesized that mixed CO/NO-releasing molecules could provide an advantageous alternative to CORMs and NORMs, as such entities should be able to deliver both gasotransmitters and thus in principle promote, or exploit, the positive feedback loop mechanism now recognized for the two diatomic molecules in higher organisms. To the best of our knowledge, a chemical approach to these types of molecules has not yet been described.

To test our hypothesis we prepared mixed CO/NO-releasing molecules from the reaction of the 17-electron organometallic CORM *cis*-[Re(CO)$_2$Br$_4$]$^{2-}$ complex with *N*-nitrosamine functionalized cyanocobalamin (B12) bio-vectors. The design of the molecules was based on previous findings published by our group. Indeed in the last few years we have shown that d^5

[a]*Department of Chemistry, University of Zürich, Winterthurerstrasse 190, CH-8057 Zürich, Switzerland*
[b]*Department of Chemistry, University of Fribourg, Chemin du Musée 9, CH-1700 Fribourg, Switzerland. E-mail: fabio.zobi@unifr.ch; Fax: (+41) 026 300 9738; Tel: (+41) 026 300 8785*
[c]*Institute of Veterinary Physiology, University of Zürich, Winterthurerstrasse 260, CH-8057 Zürich, Switzerland*

†Electronic supplementary information (ESI) available: Crystal data and structure refinement for **1** and **1a**; ^{1}H-NMR, UV-Vis, HPLC, IR and high-resolution MS spectra of molecules. CCDC 1054820 and 1054821. For ESI and crystallographic data in CIF or other electronic format

carbonyl Re complexes possess features which make them attractive as CORMs[24,25] and if appended to B12 are able to aid the differentiation of embryonic stem cells into energetically-efficient cardiomyocytes which may contribute to functional repair in progressive degenerative cardiac diseases.[26,27] In this contribution we report the synthesis and characterization of the above mentioned mixed CO/NO-releasing molecules and the cytoprotective effects of the same tested on cultured 3T3 fibroblasts under conditions of ischemia–reperfusion mimicking settings. While all molecules show cytoprotection in our model, no significant enhanced synergistic effects over the relative NORMs and CORMs building constituents were observed.

Results and discussion

Synthesis and characterization of compounds

With the long-term aim of applying the molecules *in vivo*, we selected as a biocompatible scaffold for our chemistry, cyanocobalamin. NO-releasing molecules (NORMs **1a**, **2a** and **3a**, Scheme 1) were first obtained by *N*,*N*-carbonylditriazole (CDT) amide coupling of the desired macrocycle on the ribose 5′-OH functionality, followed by $NaNO_2$ nitrosation to the corresponding *N*-nitrosamines. Overall, this procedure affords reasonable yields, but the efficiency of the reaction is rather poor, particularly in the case of hexacyclen. Specifically, we found that the critical synthetic step is the first amide coupling with typical isolated yield of *ca.* 70, 40 and 15% for pyrazine, tetraazacyclodecane and hexacyclen respectively. Conversely, nitrosation affords complete conversion of the precursors to species **1a**, **2a** and **3a**. Mixed CO/NO-releasing molecules (**1b**, **2b** and **3b** in Scheme 1) were finally isolated following conjugation of the 17-electron *cis*-$[Re(CO)_2Br_4]^{2-}$ anion to the axial cyano group of derivatives **1a**, **2a** and **3a**.[26] Coordination of the organometallic species was confirmed by the hypsochromic shift of the νCN stretching frequency (typical of these metal conjugates)[28–31] and the presence of characteristic νCO bands in infrared spectra of **1b**, **2b** and **3b**. Inductively coupled plasma/optical emission spectrometry further confirmed the expected percentage concentration of rhenium in the species, calculated as the fraction of the weight of the samples.

All species were characterized by standard analytical techniques, including X-ray crystallography for **1** and **1a** (see Fig. 1 and 2 respectively and ESI† for crystallographic details). Compound **1** crystallized in the $P2_12_12_1$ space group (typical for B12 species) and showed no significant structural differences when compared to B12. Due to low diffraction of the crystals, and the presence of 11 disordered H_2O solvent molecules the R_1 value for this species is relatively high when compared to other B12-based solid-state structures (10.4% *vs.* 7–9% on average, see the Experimental section for further details). Compound **1a** crystallized as a dimer in the $P2_1$ space group, a rare example of a vitamin B12 monomer whose solid state structure is not found in $P2_12_12_1$ (Fig. 2).[32–35] The pyrazine rings in both molecules of the unit cell were found to be disordered, probably due to different conformations imposed by the high N–NO rotational barrier.[36,37] Interestingly, the NO bond lengths are different in the two molecules. These are 1.096 (13) and 1.217 (14) for atoms labelled N17–O16 and N34–O32 respectively in Fig. 2. This dimer may persist in solution as revealed by the splitting of the pyrazine resonances evidenced by ^{1}H-NMR spectroscopy (Fig. 2, ESI†). In general, in comparison

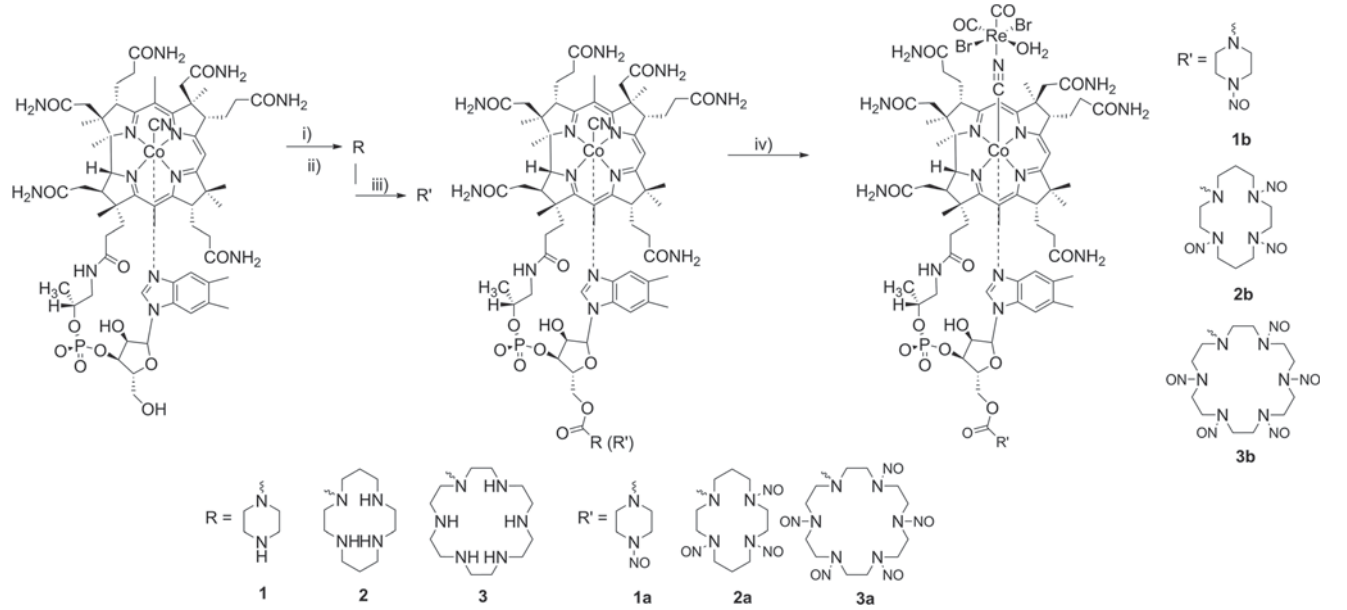

Scheme 1 Synthetic procedure to mixed CO/NO-releasing molecules. Conditions are: (i) DMSO, CDT, 12 h, 60 °C followed by (ii) selected macrocycle; (iii) AcOH, $NaNO_2$, 2 h, RT; (iv) MeOH, $[Et_4N]_2[Re(CO)_2Br_4]$, N2, 1 h, RT.

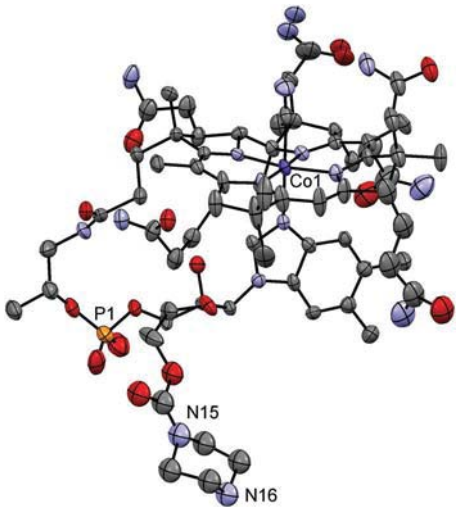

Fig. 1 X-ray structure of compound **1** with thermal ellipsoids drawn at 30% probability. Hydrogen atoms are omitted for clarity. Crystallographic details are summarized in the ESI.†

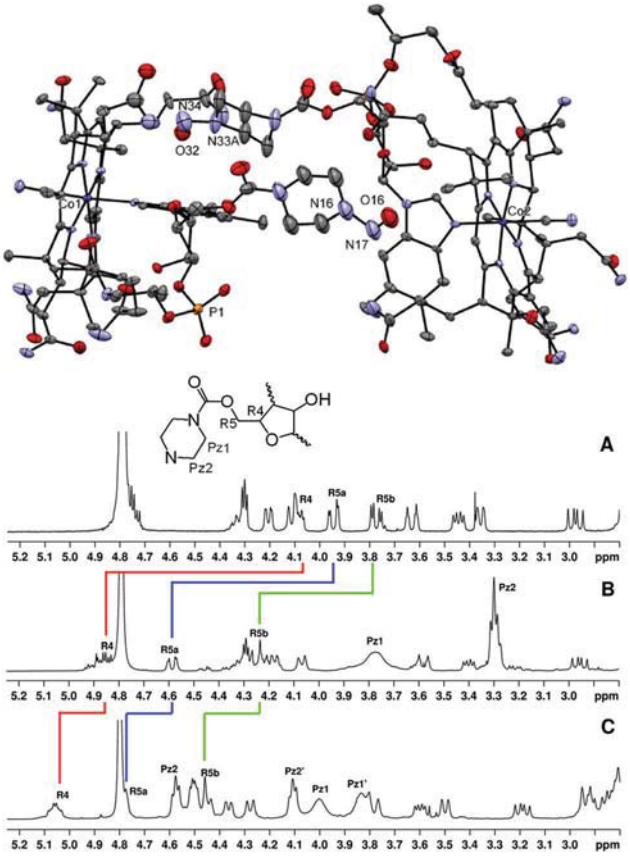

Fig. 2 X-ray structure (top) of compound **1a** with thermal ellipsoids drawn at 30% probability. Hydrogen atoms are omitted for clarity. Crystallographic details are summarized in the ESI.† ^{1}H-NMR (5.25–3.8 ppm, D_2O, 298 K of (A) vitamin B12, (B) species **1** and (C) species **1a**. Peaks labeled Pz# refer to resonances of pyrazine, while R4, R5a and R5b are those of the ribose sugar (see the text further details).

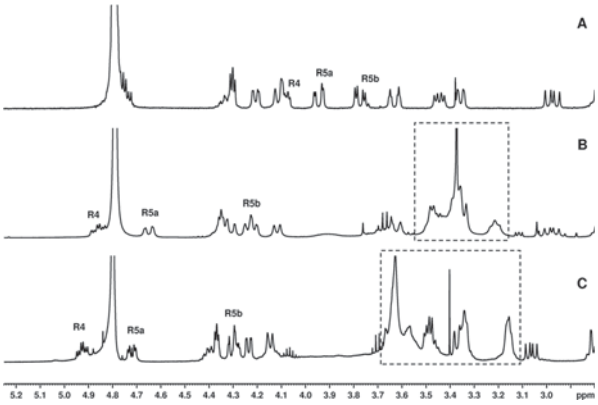

Fig. 3 ^{1}H-NMR (5.25–3.8 ppm, D_2O, 298 K) of (A) vitamin B12, (B) species **2** and (C) species **3**. Signals enclosed in segmented boxes are those of 1,4,8,11-tetraazacyclotetradecane (**tacd**) and hexacyclen (**hacd**) respectively. Peaks labeled R4, R5a and R5b refer to resonances of the ribose sugar.

with the free vitamin, the most significant feature observed in the ^{1}H-NMR spectra of these species, is a progressive shift to lower magnetic field of the ribose R4, R5a and R5b protons as a consequence of amide coupling of the heterocycles and their subsequent nitrosation. Furthermore, resonances of the heterocycles appear as broad signals which can be attributed to their fluxionality and possibly to tautomerization and interconversion of the anchoring nitrogen between its amide and imidic acid forms. To illustrate these features Fig. 3 shows the comparison of the ^{1}H-NMR spectra of B12, **2** and **3**. The shifts of the ribose protons and the broad heterocycle resonances are clearly seen.

CO and NO releasing properties of 1a–3a and 1b–3b

The CO releasing profile of the *cis*-$[Re(CO)_2Br_4]^{2-}$ species were previously reported and herein confirmed for **1b**, **2b** and **3b** (see the ESI† for a typical spectrum).[26,38] The nitric oxide releasing properties of molecules **1a**, **2a** and **3a** were also evaluated *via* the well-known myoglobin assay.[39] The assay consists of monitoring *via* UV-visible spectroscopy the conversion of deoxy-myoglobin (deoxy-Mb) with a maximum absorption peak of the Q band at 560 nm, to carboxy-myoglobin (Mb-CO) or nitrosyl-myoglobin (Mb-NO) which show two absorption maxima in the 540–548 and 575–580 nm for the same band.[40]

The reaction between deoxy-Mb and NO was initiated by adding a small aliquot of a freshly prepared concentrated aqueous solution of either **1a**, **2a** or **3a** to a Mb solution in phosphate buffer (0.1 M, pH 7.4) previously treated with sodium dithionite[41] (final concentrations: 12 μM deoxy-Mb and 50 μM for NORM's). Incubation of the deoxy-Mb solution with **1a** caused little spectroscopic change over a 5 h monitoring period, indicating that the molecule is a poor NO releaser. However, when **2a** or **3a** was used in the same assay, the deoxy-Mb spectrum evolved with the expected spectral changes associated with NO release (Fig. 4). Under the experimental conditions Mb-NO concentration reached a maximum within

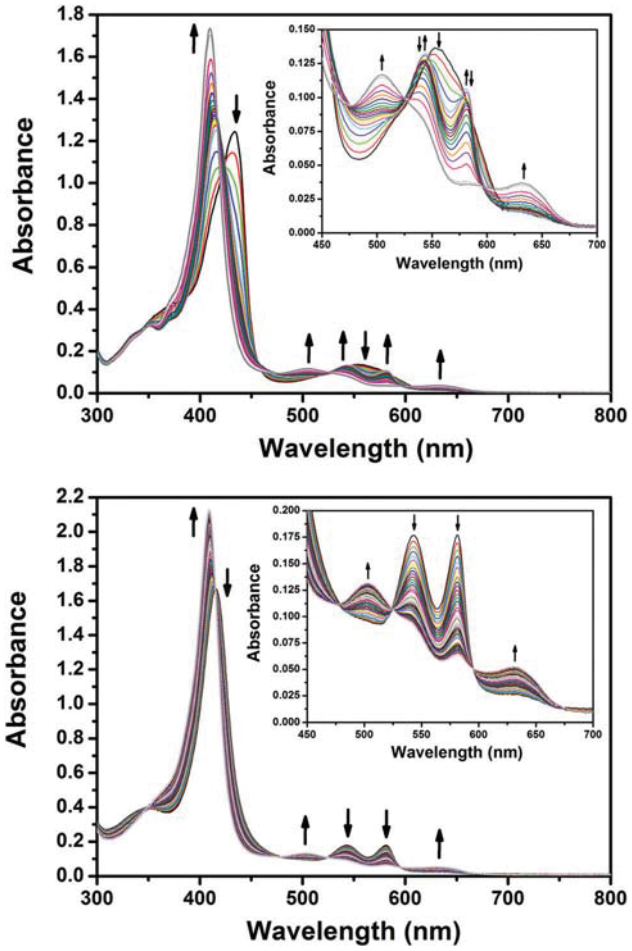

Fig. 4 Spectrum changes of a deoxy-Mb (top) and an oxy-Mb (bottom) solution (both 12 μM) incubated with a 50 μM solution of **3a** over a 24 h period (1 h intervals). Arrows indicate the relative spectroscopic variations. Insets detail changes of the Q band. In the top figure insert, the initial growth of Mb-NO (over *ca.* 5 h) is followed by its disappearance and conversion to met-Mb (over remaining 19 h). See the text for further details.

5 h of incubation. After this time, the two Mb-NO absorption maxima at 548 and 583 nm began to steadily decrease while peaks at 505 and 630 nm increased in intensity. The changes are associated with the conversion of Mb-NO to metmyoglobin (met-Mb), due to slow oxygen dissolution in the reaction medium.

In the presence of dioxygen, nitric oxide can catalyze the oxidation of Mb to met-Mb through the formation of a peroxynitrite derivative (referred to as met-Mb(OONO)).[42–44] This species is also generally assumed to be the first intermediate of the reaction between oxy-myoglobin (oxy-Mb) and NO. In order to understand if **2a**-, **3a**-derived NO could also elicit the spectroscopic changes linked to oxy-Mb to met-Mb conversion, a fresh solution of oxy-Mb was prepared according to the method of Bauer and Pacyna and incubated with the molecules.[45] As shown in Fig. 4 **3a**-derived NO provided a clean conversion between the two Mb species. In the presence of **3a**, the two absorption maxima of oxy-Mb at 542 and 579 nm steadily decreased over a 24 h period while the met-Mb peaks at 505 and 630 nm increased. A total of five isosbestic points at 350, 411, 478, 524 and 580 nm accompanied the conversion.

The total amount of NO released by **1a–3a** and **1b–3b** was determined by reductive gas-phase chemiluminescence detection in PBS buffer and in cell culture medium overlaying the monolayer of 3T3 fibroblasts (data relative to 100 μM solutions, see Table 1 and Fig. 5).[46,47] The method entails the oxidation of all NO_x species in solution to NO_3^- followed by its step-wise reduction to NO_2^- and NO which is finally carried in a He flow and allowed to interact with O_3 in a reaction chamber. The ensuing reaction is then followed by light emission detected by a photomultiplier (see Experimental for further details). For species **1a–3a** in PBS, **3a** released the highest total detectable amount of NO, *ca.* 7 μM, while **1a** and **2a** released about half the same amount. Similar results were found in cell culture. In this case, however, the total amount of NO released by **2a** and **3a** was twice that determined in PBS (*ca.* 7 and 15 μM respectively) while it was constant for **1a**. Thus, it appears that **2a** and **3a** are activated by cultured 3T3 fibroblast towards NO liber-

Table 1 Amount of nitric oxide released by **1a–3a** and **1b–3b** (100 μM solutions) in PBS buffer and 3T3 cell culture after 30 h of incubation

	PBS total (μM)	Cell culture total (μM)
1a	3.7 ± 0.4	4.1 ± 0.9
2a	3.2 ± 0.6	6.9 ± 0.5
3a	7.1 ± 1.1	14.9 ± 2.0
1b	3.9 ± 0.3	4.4 ± 0.8
2b	3.6 ± 0.7	7.7 ± 0.4
3b	8.7 ± 0.9	19.0 ± 1.8

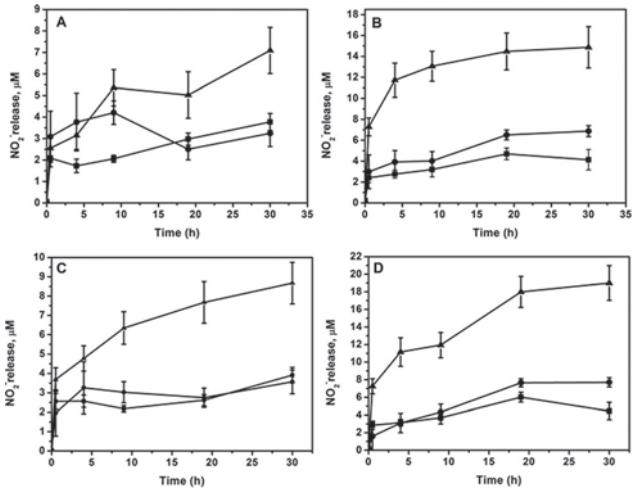

Fig. 5 Reductive gas-phase chemiluminescence detection of NO released by 100 μM solutions: of **1a** (■), **2a** (●) and **3a** (▲) in (A) PBS buffer (pH 7.4) and (B) 3T3 cell culture and of **1b** (■), **2b** (●) and **3b** (▲) in (C) PBS buffer (pH 7.4) and (D) 3T3 cell culture.

ation, with relative total concentrations of released NO comparable to other *N*-nitrosamine derivatives.[36,37] Mixed CO/NO molecules **1b–3b** released comparable amounts of NO, with **3b** giving the highest total measured concentration of the gas (*ca*. 20 μM, Table 1).

Cytoprotective properties of 1a–3a and 1b–3b

The cytoprotective properties of mixed CO/NO-releasing molecules **1b**, **2b** and **3b** were tested in an ischemia–reperfusion model on the 3T3 fibroblast cell culture and compared to NORMs **1a**, **2a** and **3a** and the CO-releasing molecule B12-ReCORM-2 (Fig. 6).[26] The latter afforded the pure CORM-only model for direct comparison to the species herein described. Compounds were administered at reperfusion at a 30 μM concentration and responses of cells to metabolic depletion were measured after 48 h as reflected in the percentage of dead cells in the monolayer. Identical sets of experiments were performed with two sets of samples, one of which was treated with freshly-dissolved compounds (blue bars in Fig. 6) and the other with compounds, which were in aqueous solution for more than 50 h to release all the gaseous molecules (orange bars in Fig. 6). B12-ReCORM-2 was used to assess the possible additivity of NO and CO for protection from ischemia–reperfusion injury. As followed from Fig. 6, the number of dead cells reduced when cells were treated with any of gas-emitting compounds compared to that in the non-treated control (grey bar). The protective effect was lost when compounds were administered after they released the gases (orange bars). The presence of NO did not result in any additional protection than that provided by B12-ReCORM-2 alone. In agreement with our previous findings,[48] protection accomplished by the combined CO/NO-releasing compounds was associated with prevention from de-attachment of 3T3 cells from the bottom of the petri-dish and reduction of stress fiber formation. No other significant morphological changes could be observed in 3T3 cells treated with our compounds (Fig. 7). The lack of additional cytoprotective effects of NO when applied along with CO suggests that both gases may share similar pathways of cytoprotection in our experimental settings.[49]

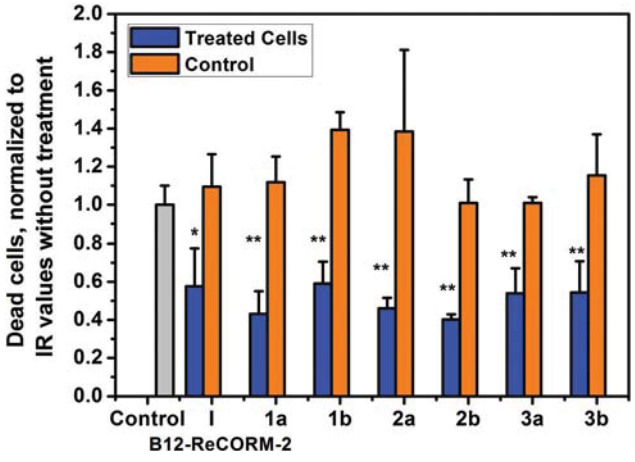

Fig. 6 Effects of active (blue) and inactive (orange) B12 species **1a**, **2a**, **3a** and **1b**, **2b**, **3b** on the viability of fibroblasts in cell cultures under in an ischemia–reperfusion model. Non-treated control is shown in grey. Data are means of 8 experiments ±SEM. B12 species concentration is 30 μM; incubation time 48 h (see the ESI† for details). * and ** stand for $p < 0.05$ and $p < 0.01$ compared to the non-treated control.

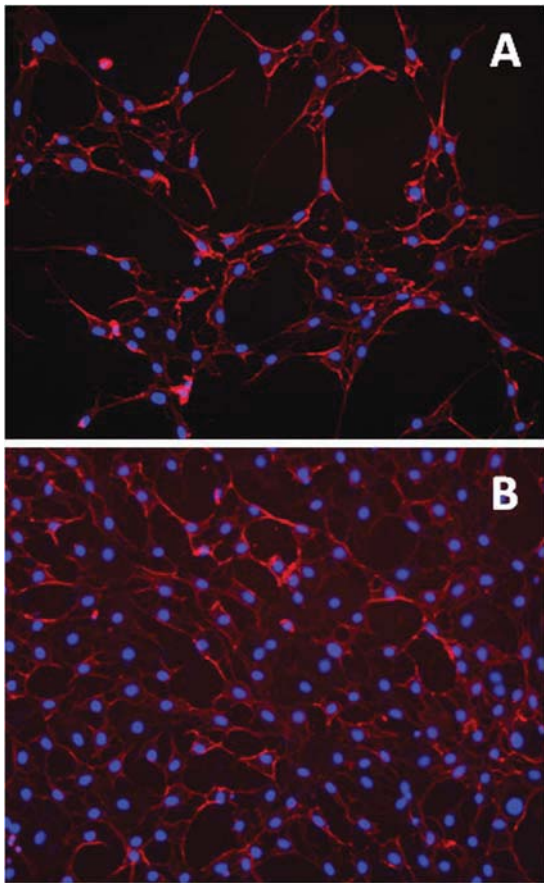

Fig. 7 (A) Representative histochemical staining of (A) untreated 3T3 fibroblasts (control) and (B) the cells treated with 30 μM **3b**. Stained in blue (DAPI) are the nuclei, actin filaments (phalloidin) are shown in red.

Conclusions

In summary, we have presented in this contribution the synthesis and characterization of the first examples of mixed CO/NO-releasing molecules based on *N*-nitrosamine-{*cis*-Re-$[CO]_2\}^{2+}$ cobalamin conjugates. The derivatives were shown to be able to release both gases, albeit NO in relatively small doses. When tested in an ischemia–reperfusion model on 3T3 fibroblast cell cultures, all species afforded cytoprotection but we found no significant enhanced synergistic effects over the relative NORMs and CORMs alone. Despite the lack of enhanced cytoprotection exhibited by the mixed CO/NO-releasing molecules in the specific model we selected, we believe this new class of compounds may be possibly considered as alternative therapeutic agents along classical NORMs and CORMs.

Experimental

Chemicals and solvents were purchased from standard sources. Chemicals were of reagent grade and used as purchased without further purification. Solvents were of reagent grade or distilled under anaerobic conditions. Water was doubly distilled before use. Reactions in a glove box were performed with solvents which were dried and deoxygenated by stirring and refluxing under a nitrogen atmosphere over the appropriate drying agent and, subsequently, distilled off. Degassed (not dried) solvents were prepared by freeze–thaw cycles or by sonication under vacuum. All synthetic work was carried out under a nitrogen atmosphere using standard Schlenk techniques. Experiments involving myoglobin and reactions where the CDT coupling was required were prepared in a glove box (Siemens MBraun Labmaster DP) with N_2 as a working gas and automatic oxygen and moisture purifier. Reaction controls were conducted *via* HPLC (default gradient as described in method 1, *vide infra*).

Elemental analyses (EA) were performed on a Leco CHNS-932 elemental analyzer. For EA measurements, samples of the vitamin B12 species were purified *via* HPLC, lyophilized and subjected to high vacuum for 7 days. Often deviations from expected values were recorded. In these cases addition of vanadium pentoxide (V_2O_5) improved the results. UV-visible spectra were performed using a Cary 50 spectrometer, with 1 cm^3 quartz cells. Cuvettes were adapted with silicon septa lids which ensured that samples were maintained under an inert atmosphere. ESI-MS measurements were performed on a Bruker Esquire HCT (ESI) instrument. The solvent flow rate was 5 μl min^{-1}, a nebulizer pressure of 15 psi and a dry gas flow rate of 5 L min^{-1} at a dry gas temperature of 300 °C were used. NMR spectra were recorded on Bruker AV2-400, AV2-500 and Bruker DRX-500 spectrometers (^{1}H at 400 MHz and 500 MHz respectively). Chemical shifts are reported relative to residual solvent resonance. Inductively coupled plasma/optical emission spectrometry (ICP/OES) measurements were performed on a Perkin Elmer Optima 7300 V HF ICP-OES Spectrometer.

Analytical HPLC methods

Method 1. Hitachi LaChrom L-7000 instrument. Column: Macherey-Nagel, EC250/3 Nucleosil 100-5 C18. Flow rate 0.5 mL min^{-1}. Absorbance monitored at 250 nm. Solutions: A: 0.1% trifluoroacetic acid in water; B: methanol. Chromatographic method: 0–5 min: isocratic flow of 75% A–25% B (A = TFA 0.1% in water; B = methanol); 5–40 min: linear gradient to 100% methanol. *Method 2*. Hitachi LaChrom L-7000 instrument. Column: Nucleodur 100-5 C18. Flow rate 0.5 mL min^{-1}. Absorbance monitored at 250 nm. Solutions: A: 0.1% trifluoroacetic acid in water; B: methanol. Chromatographic method: 0–5 min: isocratic flow of 90% A–10% B; 5–35 min: linear gradient to 100% B; 35–40 min: isocratic flow of 100% B.

Preparative HPLC method

Preparative HPLC purifications were run either on a Varian Pro Star or a Hitachi LaChrom L-7000 instrument using a Nucleodur C18 Gravity column. Gradient used: A: 0.1% trifluoroacetic acid in water; B: methanol; flow rate = 30 ml min^{-1}; 0–10 min 75% A, 10–110 min 25–100% B.

Crystal structure determination

X-ray analyses were performed at 183(2) K on an Agilent Technologies Xcalibur diffractometer with a Ruby detector[50] using a single wavelength Enhance X-ray source with Mo Kα radiation (λ = 0.71073 Å) from a micro-focus X-ray source and an Oxford Instruments Cryojet XL cooler. Suitable crystals were covered with oil (Infineum V8512, formerly known as Paratone N). Pre-experiment, data collection, data reduction and absorption correction were performed with the program suite CrysAlisPro.[51] Using Olex2,[52] the structures were solved with the ShelXS-97 [53] structure solution program and refined with the SHELXL-2014/6 [54] program package by full-matrix least-squares minimization on F^2. Isolated solvent molecules could be identified around the main species but could not be included in the refinement cycles due to serious disorders. With the use of the PLATON SQUEEZE tool,[55] their contribution was calculated as 432 electrons within the cell of **1** and attributed to 44 water molecules (11 molecules per asymmetric unit with Z = 4) and 522 electrons within the cell of **1a** attributed to 2 acetone molecules and 46 water molecules (1 and 23 solvent molecules per asymmetric unit with Z = 2, respectively). CCDC-1054820 (for **1**) and CCDC-1054821 (for **1a**) contain the supplementary crystallographic data for this paper.

Synthesis of compounds 1–3

In a round-bottom flask cyanocobalamin (100 mg, 0.074 mmol) was dissolved in 1–5 ml of dry DMSO. A total of 25 mg of *N*,*N*-carbonylditriazole (CDT, 0.15 mmol) was added and the resulting mixture was heated to 60 °C for 12 h with constant stirring. The solution was allowed to cool to RT and then a total of 1 mmol of the heterocyclic compound of interest (*i.e.* pyrazine = **pz**, 1,4,8,11-tetraazacyclotetradecane = **tacd** and hexacyclen = **hacd** for **1**, **2** and **3** respectively) was added. The mixture was stirred for 12 h at RT and then slowly added to a rapidly stirring mixture of 150 mL 1 : 1 diethyl ether : chloroform. The red precipitate was collected by vacuum filtration, washed with 30 mL of acetone and vacuum dried. The resulting red powder was then purified by preparative HPLC. ***Note***: for the synthesis of **3**, best results are obtained by using 1 ml of dry DMSO.

Analytical data for **1**: yield 89 mg, 76%. HPLC (method 1): retention time 14.9 min. ESI-MS analysis (positive mode) m/z = 1467.1 [M^+]. ^{1}H NMR (400 MHz, D_2O) δ/ppm = (a) (B12 resonances) 0.36 (s, 3H), 1.09 (s, 3H), 1.16 (d, 3H), 1.29 (s, 3H), 1.31 (s, 3H), 1.34 (s, 3H), 1.76 (s, 3H), 2.15 (d, 6H), 2.45 (s, 3H), 2.48 (s, 3H), 1.00–4.26 (m's, 31H), 4.52 (d, 1H), 4.87–4.76 (m, 3H), 5.98 (s, 1H), 6.23 (d, 1H), 6.41 (s, 1H), 6.99 (s, 1H), 7.15 (s, 1H); (b) (pz resonances) broad overlapped signals 3.71–3.23

(m, 20H). I.r. (solid state, KBr, cm^{-1}): $\nu_{C\equiv N}$ 2134. Elemental Anal. Calcd for $C_{68}H_{96}CoN_{16}O_{15}P$ (1467.49), C 55.65%, H 6.59%, N 15.27%. Found: C 54.68%, H 6.76%, N 14.77%. Single crystals suitable for X-ray diffraction analysis were grown by slow diffusion of acetone into an aqueous solution of **1**.

Analytical data for **2**: yield 50 mg, 46%. HPLC (method 1): retention time 13.3 min. ESI-MS analysis (positive mode) m/z = 1582.4 [M + H^+]. ^{1}H NMR (500 MHz, MeOD) δ/ppm = (a) (B12 resonances) 0.42 (s, 3H), 1.17 (s, 3H), 1.23 (d, 3H), 1.34 (s, 3H), 1.36 (s, 3H), 1.43 (s, 3H), 1.86 (s, 3H), 2.26 (d, 6H), 2.51 (s, 3H), 2.56 (s, 3H), 1.00–2.63 (m's, 24H), 3.64 (m, 4H), 4.11 (d, 1H), 4.55–4.20 (m, 6H), 6.05 (s, 1H), 6.32 (d, 1H), 6.57 (s, 1H), 7.07 (s, 1H), 7.22 (s, 1H); b) (tacd resonances) broad overlapped signals 3.45–3.10 (m's, 20H). I.r. (solid state, KBr, cm^{-1}): $\nu_{C\equiv N}$ 2134. Elemental Anal. Calcd for $C_{74}H_{110}CoN_{18}O_{15}P$ (1581.68), C 56.19%, H 7.01%, N 15.94%. Found: C 54.17%, H 7.26%, N 15.08%.

Analytical data for **3**: yield 20 mg, 19%. HPLC (method 1): retention time 13.7 min. ESI-MS analysis (positive mode) m/z = 1639.9 [M + H^+]. ^{1}H NMR (500 MHz, D_2O) δ/ppm = (a) (B12 resonances) 0.42 (s, 3H), 1.16 (s, 3H), 1.24 (d, 3H), 1.35 (s, 3H), 1.37 (s, 3H), 1.41 (s, 3H), 1.83 (s, 3H), 2.23 (s, 6H), 2.51 (s, 3H), 2.55 (s, 3H), 1.00–2.63 (m's, 22H), 2.97 (dd, 1H), 3.16 (d, 1H), 3.29 (dt, 2H), 3.45 (m, 1H), 3.58 (dd, 1H), 3.71 (t, 2H), 3.97 (d, 1H), 4.17–4.07 (m, 3H), 4.30 (dd, 1H), 6.05 (s, 1H), 6.32 (d, 1H), 6.47 (s, 1H), 7.03 (s, 1H), 7.19 (s, 1H); (b) (edac resonances) broad overlapped signals 3.54–3.16 (m, 24H). I.r. (solid state, KBr, cm^{-1}): $\nu_{C\equiv N}$ 2134. Elemental Anal. Calcd for $C_{76}H_{116}CoN_{20}O_{15}P$ (1639.77), C 55.67%, H 7.13%, N 17.08%. Found: C 53.32%, H 7.30%, N 16.63%.

Synthesis of compounds 1a–3a

The following general synthetic procedure was applied. In a round-bottom flask with a side arm 0.012 mmol of either **1**, **3** or **5** were dissolved in 3 ml of acetic acid. A total of 100 mg of $NaNO_2$ (1.45 mmol) was added and the flask was sealed. NO gas began to evolve immediately. The mixture was stirred at room temperature for 2 hours and then the solution was dried under reduced pressure. The red solid was then purified by preparative HPLC. **Caution**: During the procedure an over-pressure builds inside the reaction vessel. All precautions should be taken to avoid possible explosions.

Analytical data for **1a**: yield 13.7 mg, 71%. HPLC (method 2): retention time 20.4 min. ESI-MS analysis (positive mode) m/z = 1519.0 [M + Na^+]. ^{1}H NMR (400 MHz, D_2O) δ/ppm = (a) (B12 resonances) 0.63 (s, 3H), 1.37 (s, 3H), 1.42 (d, 3H), 1.57 (s, 3H), 1.58 (s, 3H), 1.61 (s, 3H), 2.04 (s, 3H), 2.44 (s, 6H), 2.71 (s, 3H), 2.74 (s, 3H), 1.14–4.46 (m's, 32H), 4.50 (m, 2H), 5.06 (m, 1H), 6.23 (s, 1H), 6.47 (d, 1H), 6.69 (s, 1H), 7.28 (s, 1H), 7.43 (s, 1H); (b) (pz resonances) broad signals 4.58 (m, 2H), 4.11 (m, 2H), 4.00 (broad, 2H), 3.83 (broad, 2H). I.r. (solid state, KBr, cm^{-1}): $\nu_{C\equiv N}$ 2134. UV-Vis (nm, MeOH, ε: cm^{-1} M^{-1}): 360 (20 334), 397 (4882), 521 (6510), 545 (6533). Elemental Anal. Calcd for $C_{68}H_{93}CoN_{17}O_{16}P$ (1496.49), C 54.58%, H 6.40%, N 15.91%. Found: C 53.83%, H 6.64%, N 15.52%. Single crystals suitable for X-ray diffraction analysis were grown by slow diffusion of acetone into an aqueous solution of **1a**.

Analytical data for **2a**: yield 15.4 mg, 77%. HPLC (method 2): retention time 21.7 min. ESI-MS analysis (positive mode) m/z = 1691.3 [M + Na^+]. I.r. (solid state, KBr, cm^{-1}): $\nu_{C\equiv N}$ 2134. UV-Vis (nm, MeOH, ε: cm^{-1} M^{-1}): 361 (19 050), 399 (3779), 519 (5635), 549 (6230). Elemental Anal. Calcd for $C_{74}H_{107}CoN_{21}O_{18}P$ (1668.68), C 53.26%, H 6.46%, N 17.63%. Found: C 51.04%, H 6.66%, N 17.05%.

Analytical data for **3a**: yield 16 mg, 75%. HPLC (method 2): retention time 14.6 min. ESI-MS analysis (positive mode) m/z = 1806.8 [M + Na^+]. I.r. (solid state, KBr, cm^{-1}): $\nu_{C\equiv N}$ 2134. UV-Vis (nm, MeOH, ε: cm^{-1} M^{-1}): 361 (20 976), 400 (3238), 518 (5991), 548 (6721). Elemental Anal. Calcd for $C_{76}H_{111}CoN_{25}O_{20}P$ (1784.76), C 51.14%, H 6.27%, N 19.62%. Found: C 48.95%, H 6.52%, N 18.93%.

Contrary to that observed for **1**, nitrosation of **2** and **3** gave derivatives (*i.e.* **2a** and **3a**) whose NMR spectra were severely complicated not only by the different conformations of the pending **tacd** and **hacd** but also from an equilibrium between the base-on/off forms of the vitamin (spectra not shown). Despite our efforts, we could not unambiguously assign specific sets of resonances.

Synthesis of compounds 1b–3b

The following general synthetic procedure was applied. In a round-bottom flask with a side arm 10 mg of either **1a**, **2a** or **3a** and 10 mg of the $[Et_4N]_2[Re(CO)_2Br_4]$ salt were added as solids under nitrogen.[24] A total of 6 ml of degassed methanol was added giving a dark purple solution, stirred and then the flask was lowered into an oil bath preheated to 50 °C. The temperature was maintained constant for 1 h and then lowered to 40 °C within 30 min. Heating was stopped and the solvent removed under reduced pressure. The resulting dark red powder was washed several times with CH_2Cl_2, acetone and then again with CH_2Cl_2 until washings (containing a mixture of unreacted $[Et_4N]_2[Re(CO)_2Br_4]$ and $(Et_4N)Br$) were clear.

Analytical data for **1b**: HPLC: retention time 30.5 min. I.r. (solid state, KBr, cm^{-1}): $\nu_{C\equiv O}$ 1986, 1890; $\nu_{C\equiv N}$ 2181. HR-ESI-MS analysis (positive mode) m/z Calcd = 1900.4171; Found: 1900.4190. UV-Vis (nm, MeOH, ε: cm^{-1} M^{-1}): 360 (19 626), 400 (5487), 520 (6117), 545 (6158). Elemental Anal. Calcd for $C_{71}H_{99}Br_2CoN_{17}O_{19}PRe$ (1930.57), C 44.17%, H 5.17%, N 12.33%. Found: C 46.29%, H 6.37%, N 11.57%. ICP/OES measurements of Re content by relative weight: calcd 9.65; found 9.28 ± 0.12.

Analytical data for **2b**: HPLC: retention time 32.7 min. I.r. (solid state, KBr, cm^{-1}): $\nu_{C\equiv O}$ 1990, 1841; $\nu_{C\equiv N}$ 2183. HR-ESI-MS analysis (positive mode) m/z Calcd = 2071.5055; Found: 2071.5178. UV-Vis (nm, MeOH, ε: cm^{-1} M^{-1}): 361 (19 041), 403 (4550), 519 (5349), 550 (5957). Elemental Anal. Calcd for $C_{77}H_{111}Br_2CoN_{21}O_{21}PRe$ (2102.76), C 43.98%, H 5.32%, N 13.99%. Found: C 45.89%, H 5.57%, N 12.46%.

ICP/OES measurements of Re content by relative weight: calcd 8.86; found 8.36 ± 0.24.

Analytical data for **3b**: HPLC (method 2): retention time 28.7 min. I.r. (solid state, KBr, cm^{-1}): $\nu_{C\equiv O}$ 1989, 1841; $\nu_{C\equiv N}$ 2183. HR-ESI-MS analysis (positive mode) *m*/*z* Calcd = 2187.5390; Found: 2187.5388. UV-Vis (nm, MeOH, ε: cm^{-1} M^{-1}): 361 (20 556), 408 (4500), 517 (5556), 549 (6300). Elemental Anal. Calcd for $C_{79}H_{115}Br_2CoN_{25}O_{23}PRe$ (2218.83), C 42.76%, H 5.22%, N 15.78%. Found: C 44.25%, H 5.38%, N 14.69%. ICP/OES measurements of Re content by relative weight: calcd 8.39; found 8.08 ± 0.29.

NO detection in PBS buffer and the cell culture medium in contact with 3T3 cells

NIH stock solutions (1 mM) of **1a–3a**, and **1b–3b** were prepared in sterile phosphate buffer (PBS, pH 7.4) and added either to fresh PBS buffer, culture medium which had been previously in contact with cells, or cultured cells to a final concentration of 100 μM. Aliquots (200 μL) of the resulting solutions were sampled at 4, 9, 19 and 30 h. For all collections, the samples were filtered through a short C18 column after priming with methanol (1.5 ml), and washing with distilled water (2 ml). The samples were passed through the column followed by 1 ml of PBS. Samples for each time point were prepared and handled in triplicates. Nitrite and nitrate assessments were performed as previously described.[47,48] Nitrate was quantitatively reduced to nitrite using Nitralyzer II kit (World Precision Instruments, Inc.) in which copper-coated cadmium bits were used for reduction. The samples (25, 50 or 100 μl) were injected into a helium-gassed reducing Brown's solution containing 1.62 g KI, 0.57 g I_2, 15 ml HPLC-grade water and 202 ml acetic acid warmed to 85 °C. Calibration solutions were prepared containing 0, 50, 100, 150 or 200 nM of $NaNO_2$ dissolved in distilled water. Nitrite was quantitatively reduced to NO when in Brown's solution and carried in a Helium flow to the reaction chamber of CLD88 nitric oxide analyzer (Eco-Medics Switzerland) in which NO was allowed to interact with O_3. The ensuing reaction was then followed by light emission detected by a photomultiplier. Final results obtained from samples dissolved in PBS were set as control while data obtained from the addition of **1a**, **2a** and **3a** to the medium in contact with 3T3 cells were normalized to the data obtained from the fresh culture medium alone.

Cell culturing and experimentation conditions during metabolic depletion

Two batches of NIH 3T3 Swiss Albino Mouse Fibroblast cells (ECACC Catalogue number 85022108) were cultured for 4 or 5 passages in Dulbecco's Modified Eagle Medium (DMEM) containing 5 mM glucose, 10% fetal calf serum (FCS), and penicillin–streptomycin at pH 7.4. About one million cells were plated per Petri dish of 4.5 cm^2 area and kept proliferating to near confluence at 37 °C in the presence of 95% air and 5% CO_2 as described earlier (see *e.g.* ref. 17 and 28). All cell culture materials were purchased from Invitrogen (Invitrogen, Life Technologies, Paisley, UK).

The following protocol was used to mimic conditions of ischemia–reperfusion. Ischemia was imitated by placing the cells grown to 60–70% confluence and DMEM (GIBCO® GlutaMAX™, Life Technologies, Paisley, UK) to the FCS-free glucose-deprived medium (Invitrogen, Life Technologies, Paisley, UK) and exposing them for 48 h to the atmosphere of 1% O_2, 94.8% N_2 and 5% CO_2 in the incubator HeraCell 240, Heraeus. Thereafter the starvation medium was replaced by the DMEM supplemented with 10% FCS and 5 mM glucose without or with B12 species (final concentration 30 μM), which were either freshly-dissolved or pre-dissolved for 54 h. This simulated "reperfusion" period lasted for 12 h. Stock 30 mM solutions of B12 species **1a**, **2a**, **3a** and **1b**, **2b**, **3b** were prepared in PBS.

Cell viability was then assessed by means of fluorescent microscopy. To do so the cells were stained for 10 min with a mixture of 1 μg mL^{-1} Hoechst-33342 and 10 μg mL^{-1} propidium iodide (PI) (Invitrogen, Molecular Probes) in Ca^{2+}/Mg^{2+}-free PBS (Gibco, Life Technologies, Paisley, UK). Hoechst-33342 (excitation and emission maxima of 360 and 450 nm, respectively, Invitrogen, Molecular Probes) is membrane-permeable and stains the nuclei of all cells by binding to double-stranded nuclear DNA. Membrane-impermeable PI (excitation and emission maxima of 555 and 620 nm, respectively) interacts with DNA and RNA of cells with a ruptured plasma membrane termed here as "dead". Fluorescent staining was recorded using the Axiovert 200-M fluorescent microscope and analyzed using MCID image analysis software. In each culture dish, cells were counted in 5 predetermined areas of 0.5 mm^2, totalling 2.5 mm^2 per dish, three dishes tested for each condition. Experiments were repeated four times (two 3T3 cell batches, two passages (P4 and P5) each). Data in each experiment were normalized to the viability in non-treated control samples and expressed as the means ± SEM. Statistical analysis was performed using GraphPad Instat v.3, GraphPad Software Inc. Following the normality test one-way anova was used with the Dunnett-post-test in which all data were compared to the viability of cells in non-treated control.

Additional batches of cells exposed to ischemia–reperfusion protocol with or without the NO and CO releasing compounds were prepared for staining with 4′,6-diamidino-2-phenylindole (DAPI) dihydrochloride (0.5 mg ml^{-1}) or phalloidin–rhodamine (Sigma-Aldrich, 1 : 100 in PBS). Staining was performed after washing twice with PBS, fixation with 4% paraformaldehyde, and permeabilization with 0.2% Triton X-100.

Acknowledgements

Financial support from the SNSF grant PP00P2_144700 is gratefully acknowledged.

Notes and references

1 S. H. Snyder, S. R. Jaffrey and R. Zakhary, *Brain Res. Rev.*, 1998, **26**, 167–175.

2 L. Xue, G. Farrugia, S. M. Miller, C. D. Ferris, S. H. Snyder and J. H. Szurszewski, *Proc. Natl. Acad. Sci. U. S. A.*, 2000, **97**, 1851–1855.

3 R. Foresti, J. E. Clark, C. J. Green and R. Motterlini, *FASEB J.*, 1997, **11**, 65–65.

4 R. Foresti, J. E. Clark, C. J. Green and R. Motterlini, *J. Biol. Chem.*, 1997, **272**, 18411–18417.

5 M. J. Alcaraz, A. Habib, M. Lebret, C. Creminon, S. Levy-Toledano and J. Maclouf, *Br. J. Pharmacol.*, 2000, **130**, 57–64.

6 S. R. Thom, Y. A. Xu and H. Ischiropoulos, *Chem. Res. Toxicol.*, 1997, **10**, 1023–1031.

7 M. Kajimura, R. Fukuda, R. M. Bateman, T. Yamamoto and M. Suematsu, *Antioxid. Redox Signaling*, 2010, **13**, 157–192.

8 S. K. Choudhari, M. Chaudhary, S. Bagde, A. R. Gadbail and V. Joshi, *World J. Surg. Oncol.*, 2013, 11.

9 L. Y. Chau, *J. Biomed. Sci.*, 2015, 22.

10 P. Pacher, J. S. Beckman and L. Liaudet, *Physiol. Rev.*, 2007, **87**, 315–424.

11 S. W. Ryter, J. Alam and A. M. K. Choi, *Physiol. Rev.*, 2006, **86**, 583–650.

12 P. G. Wang, M. Xian, X. P. Tang, X. J. Wu, Z. Wen, T. W. Cai and A. J. Janczuk, *Chem. Rev.*, 2002, **102**, 1091–1134.

13 J. L. Burgaud, J. P. Riffaud and P. Del Soldato, *Curr. Pharm. Des.*, 2002, **8**, 201–213.

14 L. J. Ignarro, C. Napoli and J. Loscalzo, *Circ. Res.*, 2002, **90**, 21–28.

15 C. C. Romao, W. A. Blattler, J. D. Seixas and G. J. L. Bernardes, *Chem. Soc. Rev.*, 2012, **41**, 3571–3583.

16 S. H. Heinemann, T. Hoshi, M. Westerhausen and A. Schiller, *Chem. Commun.*, 2014, **50**, 3644–3660.

17 B. E. Mann, *Top. Organomet. Chem.*, 2010, **32**, 247–285.

18 U. Schatzschneider, *Br. J. Pharmacol.*, 2015, **172**, 1638–1650.

19 F. Zobi, *Future Med. Chem.*, 2013, **5**, 175–188.

20 S. Garcia-Gallego and G. J. L. Bernardes, *Angew. Chem., Int. Ed.*, 2014, **53**, 9712–9721.

21 R. Motterlini and L. E. Otterbein, *Nat. Rev. Drug Discovery*, 2010, **9**, 728–724.

22 B. S. Zuckerbraun, T. R. Billiar, S. L. Otterbein, P. K. M. Kim, F. Liu, A. M. K. Choi, F. H. Bach and L. E. Otterbein, *J. Exp. Med.*, 2003, **198**, 1707–1716.

23 K. G. Raman, J. E. Barbato, E. Ifedigbo, B. A. Ozanich, M. S. Zenati, L. E. Otterbein and E. Tzeng, *J. Cardiovasc. Surg.*, 2006, **44**, 151–158.

24 F. Zobi, L. Kromer, B. Spingler and R. Alberto, *Inorg. Chem.*, 2009, **48**, 8965–8970.

25 F. Zobi and O. Blacque, *Dalton Trans.*, 2011, **40**, 4994–5001.

26 F. Zobi, O. Blacque, R. A. Jacobs, M. C. Schaub and A. Y. Bogdanova, *Dalton Trans.*, 2012, **41**, 370–378.

27 H. B. Suliman, F. Zobi and C. A. Piantadosi, *Antioxid. Redox Signaling*, 2015, in press.

28 S. Kunze, F. Zobi, P. Kurz, B. Spingler and R. Alberto, *Angew. Chem., Int. Ed.*, 2004, **43**, 5025–5029.

29 S. Mundwiler, B. Spingler, P. Kurz, S. Kunze and R. Alberto, *Chem. – Eur. J.*, 2005, **11**, 4089–4095.

30 P. Ruiz-Sanchez, S. Mundwiler, A. Medina-Molner, B. Spingler and R. Alberto, *J. Organomet. Chem.*, 2007, **692**, 1358–1362.

31 P. Ruiz-Sanchez, S. Mundwiler, B. Spingler, N. R. Buan, J. C. Escalante-Semerena and R. Alberto, *J. Biol. Inorg. Chem.*, 2008, **13**, 335–347.

32 S. N. Fedosov, M. Ruetz, K. Gruber, N. U. Fedosova and B. Krautler, *Biochemistry*, 2011, **50**, 8090–8101.

33 S. Murtaza, M. Ruetz, K. Gruber and B. Krautler, *Chem. – Eur. J.*, 2010, **16**, 10984–10988.

34 K. L. Brown, S. F. Cheng, X. Zou, J. D. Zubkowski, E. J. Valente, L. Knapton and H. M. Marques, *Inorg. Chem.*, 1997, **36**, 3666–3675.

35 K. L. Brown, S. F. Cheng, J. D. Zubkowski and E. J. Valente, *Inorg. Chem.*, 1996, **35**, 3442–3446.

36 F. Karaki, Y. Kabasawa, T. Yanagimoto, N. Umeda, Firman, Y. Urano, T. Nagano, Y. Otani and T. Ohwada, *Chem. – Eur. J.*, 2012, **18**, 1127–1141.

37 M. Miura, S. Sakamoto, K. Yamaguchi and T. Ohwada, *Tetrahedron Lett.*, 2000, **41**, 3637–3641.

38 F. Zobi, A. Degonda, M. C. Schaub and A. Y. Bogdanova, *Inorg. Chem.*, 2010, **49**, 7313–7322.

39 R. Motterlini, B. E. Mann, T. R. Johnson, J. E. Clark, R. Foresti and C. J. Green, *Curr. Pharm. Des.*, 2003, **9**, 2525–2539.

40 E. Antonini and M. Brunori, *Hemoglobin and Myoglobin in Their Reactions with Ligands*, North-Holland, Amsterdam, 1971.

41 S. McLean, B. E. Mann and R. K. Poole, *Anal. Biochem.*, 2012, **427**, 36–40.

42 K. J. Koebke, D. J. Pauly, L. Lerner, X. Liu and A. A. Pacheco, *Inorg. Chem.*, 2013, **52**, 7623–7632.

43 P. C. Ford and I. M. Lorkovic, *Chem. Rev.*, 2002, **102**, 993–1017.

44 J. Su and J. T. Groves, *Inorg. Chem.*, 2010, **49**, 6317–6329.

45 C. Bauer and B. Pacyna, *Anal. Biochem.*, 1975, **65**, 445–448.

46 U. Hendgen-Cotta, M. Grau, T. Rassaf, P. Gharini, M. Kelm and P. Kleinbongard, *Methods Enzymol.*, 2008, **441**, 295–315.

47 M. Grau, U. B. Hendgen-Cotta, P. Brouzos, C. Drexhage, T. Rassaf, T. Lauer, A. Dejam, M. Kelm and P. Kleinbongard, *J. Chromatogr., B: Anal. Technol. Biomed. Life Sci.*, 2007, **851**, 106–123.

48 F. Zobi, L. Quaroni, G. Santoro, T. Zlateva, O. Blacque, B. Sarafimov, M. C. Schaub and A. Y. Bogdanova, *J. Med. Chem.*, 2013, **56**, 6719–6731.

49 H. Haugaa, H. Gomez, D. R. Maberry, A. Holder, O. Ogundele, A. M. B. Quintero, D. Escobar, T. I. Tonnessen, H. Airgood, C. Dezfulian, E. Kenny, S. Shiva, B. Zuckerbraun and M. R. Pinsky, *Crit. Care*, 2015, **19**, 184–195.

50 *Y. Agilent Technologies (formerly Oxford Diffraction)*, Oxfordshire, England, 2012.

51 *Agilent Technologies, Yarnton*, Oxfordshire, England, CrysAlisPro, 1.171.36.20 edn., 2012.

52 O. V. Dolomanov, L. J. Bourhis, R. J. Gildea, J. A. K. Howard and H. Puschmann, *J. Appl. Crystallogr.*, 2009, **42**, 339–341.
53 G. M. Sheldrick, *Acta Crystallogr., Sect. A: Fundam. Crystallogr.*, 2008, **64**, 112–122.
54 G. M. Sheldrick, *Acta Crystallogr., Sect. A: Fundam. Crystallogr.*, 2015, **71**, 3–8.
55 A. L. Spek, *Acta Crystallogr., Sect. C: Cryst. Struct. Commun.*, 2015, **71**, 9–18.